Redox Biology 71 (2024) 103088

Contents lists available at ScienceDirect

Redox Biology

journal homepage: www.elsevier.com/locate/redox

Inhibition of ALK3-mediated signalling pathway protects against acetaminophen-induced liver injury

Patricia Marañón [a,**], Esther Rey [a,1], Stephania C. Isaza [a,1], Hanghang Wu [b], Patricia Rada [c,d], Carmen Choya-Foces [a], Antonio Martínez-Ruiz [a,e], María Ángeles Martín [d,f], Sonia Ramos [d,f], Carmelo García-Monzón [a], Francisco Javier Cubero [b,g,h], Ángela M. Valverde [c,d], Águeda González-Rodríguez [c,d,*]

[a] Unidad de Investigación, Hospital Universitario Santa Cristina, Instituto de Investigación Sanitaria Princesa (IIS-IP), Madrid, Spain
[b] Department of Immunology, Ophthalmology and ENT, Complutense University School of Medicine, Madrid, Spain
[c] Instituto de Investigaciones Biomédicas Sols-Morreale (Centro Mixto CSIC-UAM), Madrid, Spain
[d] Centro de Investigación Biomédica en Red de Diabetes y Enfermedades Metabólicas Asociadas (CIBERDEM), Madrid, Spain
[e] Departamento de Bioquímica y Biología Molecular, Facultad de Farmacia, Universidad Complutense de Madrid, Spain
[f] Instituto de Ciencia y Tecnología de Alimentos y Nutrición (ICTAN-CSIC), Madrid, Spain
[g] Instituto de Investigación Sanitaria Gregorio Marañón (IiSGM), Madrid, Spain
[h] Centro de Investigación Biomédica en Red de Enfermedades Hepáticas y Digestivas (CIBEREHD), Madrid, Spain

ARTICLE INFO

Keywords:
Acute liver failure
Drug induced liver injury
Acetaminophen
Bone morphogenetic proteins
ALK3
DMH2

ABSTRACT

Acetaminophen (APAP)-induced liver injury is one of the most prevalent causes of acute liver failure (ALF). We assessed the role of the bone morphogenetic protein (BMP) type I receptors ALK2 and ALK3 in APAP-induced hepatotoxicity. The molecular mechanisms that regulate the balance between cell death and survival and the response to oxidative stress induced by APAP was assessed in cultured human hepatocyte-derived (Huh7) cells treated with pharmacological inhibitors of ALK receptors and with modulated expression of *ALK2* or *ALK3* by lentiviral infection, and in a mouse model of APAP-induced hepatotoxicity. Inhibition of ALK3 signalling with the pharmacological inhibitor DMH2, or by silencing of *ALK3,* showed a decreased cell death both by necrosis and apoptosis after APAP treatment. Also, upon APAP challenge, ROS generation was ameliorated and, thus, ROS-mediated JNK and P38 MAPK phosphorylation was reduced in ALK3-inhibited cells compared to control cells. These results were also observed in an experimental model of APAP-induced ALF in which post-treatment with DMH2 after APAP administration significantly reduced liver tissue damage, apoptosis and oxidative stress. This study shows the protective effect of ALK3 receptor inhibition against APAP-induced hepatotoxicity. Furthermore, findings obtained from the animal model suggest that BMP signalling might be a new pharmacological target for the treatment of ALF.

1. Introduction

Drug induced liver injury (DILI) has lately become the main cause of acute liver failure (ALF), especially in Western countries, being acetaminophen (APAP) one of the main drugs causatives of DILI [1,2]. APAP is an analgesic and antipyretic drug widely used worldwide [3]. Even though it is a highly safe drug at a therapeutic dose, intentionally or unintentionally overdose can lead to ALF [4].

Hepatotoxicity occurs due to an imbalance in hepatic APAP metabolism. Glutathione (GSH) depletion caused by APAP overdose or low reserves of this peptide because of fasting or alcohol consumption among others [5], results in accumulation of the highly reactive specie NAPQI derived from APAP metabolism through the enzyme CYP2E1 [6]. NAPQI forms covalent bonds with mitochondrial proteins in hepatocytes, interfering in the electron transport chain and producing reactive oxygen species (ROS). Eventually, DNA fragmentation takes place and

* Corresponding author.Instituto de Investigaciones Biomédicas Sols-Morreale (Centro Mixto CSIC-UAM), Madrid, Spain.
** Corresponding author.
E-mail addresses: patmaranon@gmail.com (P. Marañón), aguedagr@iib.uam.es (Á. González-Rodríguez).
[1] These authors contributed equally to this work.

https://doi.org/10.1016/j.redox.2024.103088
Received 19 January 2024; Accepted 13 February 2024
Available online 15 February 2024

consequently a massive death of hepatocyte is produced [7–9].

APAP-induced liver injury is characterized by a fulminant progression, a main feature of ALF; for this reason a quick treatment is important to prevent progression and improve prognosis [10]. Nowadays, *N*-Acetyl Cysteine (NAC) is the preference treatment for patients with APAP-induced DILI; however, it has a narrow therapeutic window and has to be administrated within the first 8 h after APAP overdose [11–13]. For this reason, new pharmacologic approaches to stop up the progression of ALF are necessary.

Bone morphogenetic proteins (BMPs) are soluble growth factors that belong to the transforming growth factor (TGF) β superfamily. Regarding their signalling pathways, there are two types of serin threonine receptors involved in the signal transduction induced by BMPs in target cells [14]: type II receptors (BMPRII, ACTRIIA and ACTRIIB) which are constitutively active and can recruit and phosphorylate type I receptors (BMPRIA/ALK3, BMPRIB/ALK6, ACTRIA/ALK2 and ALK1). Although BMP ligands can bind to either type I or type II receptors, for signal transduction, ligands have to form a complex with two subunits of type I receptor and two subunits of type II receptor. Once the complex ligand-receptor is formed, the receptor subunits *trans*-phosphorylate and become active. The activated complex phosphorylates Smad1/5/8 which binds Smad 4 and translocate to the nucleus inducing the transcription of target genes. In addition, a non-canonical signalling pathway mediated by other kinases, such as PI3K and MAPK can also transduce BMP signalling [14–16].

Noteworthy, the affinity of the ligands towards BMP receptors plays a critical role in the signalling pathway triggered by these proteins [17]. It has been shown that usually this affinity is shared between the members of each subfamily of BMP proteins, since it depends on structural elements [18,19]. It has also been described that while BMP2 and BMP4 have affinity for the type I receptors ALK3 and ALK6, BMP5, 6, 7 and 8A/B have higher affinity for ALK2, and BMP9 and BMP10 signalling occurs mainly through ALK1 [20]. Thus, the transcription of different BMP target genes depends on the ligand and receptor among other factors such as the cellular type [14,21].

Previous research has demonstrated that while ALK2 and ALK3 are abundantly expressed in human liver and all hepatocyte-derived cell lines, ALK6 was not detected [21]. The relationship between BMPs and iron overload in the liver has been extensively studied, since these proteins regulate the expression of hepcidin, a key regulator of hepatic iron homeostasis [22,23]. Furthermore, a decrease of hepcidin synthesis due to BMP signalling inhibition in situation of hypoxia or oxidative stress has been observed [24,25]. Moreover, two studies have referred an increased expression of BMP2 and BMP4 in animal models of ALF [26,27]. In fact, their signalling inhibition by the knocking-down of ALK3 receptor reduced the liver capacity of repair after damage and lower expression of genes related to cell proliferation [27]. Lastly, a recent study showed that BMP signalling pathway is activated after APAP induced liver injury and is involved in tissue repair and regeneration processes upon damage [28].

To further delineate the role of BMP signalling in ALF progression, we aimed to determine the implication of BMP type I receptors ALK2 and ALK3 in APAP-induced liver injury and to assess whether pharmacological targeting on these receptors might have a beneficial effect in the treatment of ALF caused by APAP.

2. Material and methods

2.1. Cell culture and treatments

Human hepatoma cell line Huh7 (ATCC, Manassas, VA, USA) was cultured in Dulbecco's modified Eagle medium (DMEM, Cytiva, USA) with high glucose completed with Hepes, antibiotics and supplemented with 10% of fetal bovine serum (FBS). Mouse hepatocytes were isolated from male mice (8-12 weeks-old) by perfusion with collagenase and cultured as described [29]. Cells were maintained at 37 °C, 5% CO_2 and relative humidity 95%, and exposed to vehicle (ethanol) or acetaminophen (APAP, A7085 Merck Life Science, Darmstadt, Germany) for different time periods as previously described [30,31]. After treatment, plates were washed with PBS and used for further analysis.

2.2. Short hairpin ALK3 and ALK2 knockdown

A stable silencing in *ALK2* or *ALK3* genes in Huh7 cells was generated with human scrambled (ShControl, ShC) or ALK2/ALK3 ShRNA lentiviral particles (SHALK3-NM_004329.2, SHALK2-NM_001105.2 MISSION® shRNA Plasmid DNA, Merck Life Science). Briefly, HEK-293 T cell line was transfected with the corresponding lentiviral vector and packaging vectors. Lentiviral particles produced by these cells were collected and transferred to culture media containing 6 μg/ml polybrene (Santa Cruz Biotechnology Inc., Heidelberg, Germany). Huh7 cells were exposed to lentiviral particles for 24 h, and then cultured in presence of 2–5 μg/ml of puromycin (Santa Cruz Biotechnology Inc.). Resistant cells were amplified for further assays or storage and the efficiency of infection was evaluated by quantification of *ALK2* and *ALK3* gene expression by RT-qPCR, and ALK2 and ALK3 protein expression by Western Blot.

2.3. ALK2 overexpression in Huh7 cell line

A stable cell line overexpressing *ALK2* was generated using the Huh7 cell line through lentiviral infection following the protocol previously described. For this purpose, scrambled (LV Control; LV C) or ALK2 (LV ALK2 OE) lentiviral particles were used (112,920,610,395 ACVR1 (ALK2) Lentiviral Vector Human CMV, Applied Biological Materials Inc. Richmond, BC, Canada).

2.4. Pharmacological inhibition of BMP type I receptors

For specific approaches, stimulation with APAP was performed in presence of different pharmacological inhibitors of BMP type I receptors ALK2 and ALK3: LDN-193189, DMH2 and ML347 (SML-0559, Merck Life Science; 5580 and 4945, Tocris Bioscience, Minneapolis, USA). Inhibitors' affinity for each receptor and working concentration is shown in Table 1. Inhibitors were used as pre-treatment 1 h prior to APAP stimulation or 1 h after of APAP challenge.

2.5. Cell viability assessment

Cell viability was measured using crystal violet staining. Plates were washed with PBS to remove unattached dead cells and covered with 0.2% crystal violet (212120250, Thermo Fisher Scientific Inc., Madrid, Spain) diluted in 2% ethanol for 30 min. Afterwards, staining excess was removed by washing with distilled water and plates were left to dry. Finally, colorant was dissolved in 1% sodium dodecyl sulfate (SDS) and optical density was measured with spectrophotometer Spectra MR (29010, Dynex Technologies, Chantilly, USA) at 560 nm. The higher the absorbance, the higher the percentage of cell survival.

Table 1
Pharmacological inhibitors of BMP type I receptors ALK2 and ALK3.

	Ki ALK2 (nM)	Ki ALK3 (nM)	Working concentration	Control
LDN-193189	5	30	500 nM	–
DMH2	43	5.4	5 or 10 μM	DMSO
ML347	32	>200 fold selectivity	150 nM	DMSO

BMP, Bone morphogenetic protein.

2.6. Cytotoxicity assay by lactate dehydrogenase (LDH)

Cellular toxicity was evaluated by measuring lactate dehydrogenase (LDH) release to the culture media due to cellular necrosis. Assay was performed using the Cytotoxicity Detection Kit^{PLUS} LDH (0474492600, Roche Diagnostics, Mannheim, Germany) following manufacturing indications. Percentage of cytotoxicity was calculated as % of cytotoxicity = ((Sample O.D. – Control O.D.)/(Positive control O.D. – Control O.D.)) x 100.

2.7. ROS quantification in vitro by fluorescence microplate reader

Cells were seeded in a 96 multi-well plate in a density of 2x10^4 cells/plate. The probe dhihydroethidium (DHE, 2140299, Invitrogen by Thermo Fisher Scientific Inc.) was used at a concentration of 10 μM in HBSS medium complemented with glucose (4.5 g/L) and glutamine (4 mM) to measure superoxide. After 30 min with the probe, vehicle or APAP was added and ROS production was measured in a fluorescence microplate reader (CLARIOstar^{Plus} BMG Labtech, Germany) for 2 h using 488/550–580 excitation/emission filter pairs. DAPI staining was used to normalize number of cells (358/455–465). Each condition was run in triplicate and antimycin A (10 μM) was used as a positive control.

2.8. Gene expression analysis by real time quantitative PCR

Total RNA was extracted using TRIzol reagent (Vitro, Sevilla, Spain). Obtained RNA purity and concentration was measured with Nanodrop (Termofisher Nanodrop 2000c) and cDNA was obtained by reverse transcription of RNA using ImProm-II™ Reverse transcription kit (Promega Inc., Madison, WI, USA) in a T100TM Thermal Cycler (BioRad Inc., Madrid, Spain). Quantitative real time PCR (RTqPCR) was performed with SYBR Green method using StepOnePlusTM Real Time PCR System sequence detector (Thermo Fisher Scientific, Inc.) and quantified with ΔΔCt method. Samples were run in duplicate and normalized with endogenous gene *36B4*. Primer sequences are listed in Table S1.

2.9. Protein quantification by Western Blot

After *in vitro* experiments, plates were washed with PBS and cells were scraped in RIPA buffer (50 mM Tris HCl, pH 7.4, 1% Triton X-100, 0.2% SDS, 1 mM EDTA, 1 mM PMSF and 5 μg/ml leupeptin) to obtain total protein extracts. Protein samples were boiled in Laemmli buffer prior to separation in 10–15% SDS-PAGE by electrophoresis following with transferring to Immunoblot nitrocellulose membrane. After blocking, nitrocellulose membranes (Bio-Rad) were incubated overnight at 4 °C with primary antibodies: anti-phospho-Smad1 (Ser463/465)/Smad 5 (Ser463/465)/Smad 8 (Ser 426/428) (#9511), anti-Smad1 (#9512), anti-cleaved caspase 3 (#9661), anti-phospho-JNK (#4668) and anti-phospho-P38 MAPK (#9211) and anti-P38 (#9212) from Cell Signalling Technology (Danvers, MA, USA); anti-ALK2 (ACTR-I, sc-374523) and anti-JNK (D-2, sc-7345) from Santa Cruz Biotechnology Inc.; anti-ALK3 (BMPR-1A, ABD51) from Sigma-Aldrich (Madrid, Spain). Finally, membranes were incubated with the corresponding secondary antibody (Santa Cruz Biotechnology Inc.). Immunoreactive bands were visualized using the ECL Western blotting protocol (Bio-Rad). Densitometric analysis of the bands was performed using Image J software (NIH, Bethesda, USA). Anti-Tubulin (sc-166729, Santa Cruz Biotechnology Inc.), anti-vinculin (sc-73614, Santa Cruz Biotechnology Inc.) and anti-βactin antibody (A-5441, Sigma Aldrich) were used as loading control.

2.10. Animals

Mice were housed in controlled conditions of temperature (22 °C) and humidity with dark/light cycles of 12 h, fed with standard chow diet (CHD) *ad libitum* and had free access to drinking water at the animal facilities of Universidad Complutense de Madrid (UCM). All animal experimentation was carried out following both Spanish and European legislations (PROEX 125.1/20). Briefly, male C57Bl6j mice of 2 months of age were submitted to a model of APAP-induced acute liver failure as previously described [32]. APAP was firstly dissolved in DMSO and then PBS was added to a working concentration of 75 mg/ml in <1% DMSO. To ease dilution, APAP was heated to 54 °C for 1 h with shaking. Mice were fasted overnight (12 h) and then a single dose of 500 mg/kg was intraperitoneally (i.p.) injected or an equivalent dose of DMSO for controls. After 1 h, mice were treated (i.p.) with a dose of 3 mg/kg of DMH2 that was selected based on previous studies [33,34]. DMH2 was dissolved in DMSO at a concentration of 20 mM (9.1 mg/ml) and then in PBS to a working concentration of 0.3 mg/ml (DMSO 3.3%, a safe dose for the liver as previously reported [35]). Mice were sacrificed 2 or 6 h after APAP injection and livers and serum samples were collected and conveniently stored for further analysis.

2.11. Assessment of ALT activity

Blood samples were collected from animals after sacrificed and serum was used in a 1:4 dilution. ALT activity was evaluated using a colorimetric kit (41282, SPINREACT, Girona, Spain) following manufacturers' instructions.

2.12. Histopathology assessment

Livers collected from mice were fixed with 4% paraformaldehyde solution and embedded in paraffin. Then, 5 μm thick liver tissue slices were carried out. Liver sections were stained with Haematoxylin and Eosin (H&E). Images were taken using an optical microscope Nikon Eclipse E400 (Nikon, Tokyo, Japan) equipped with a plan Apocromatic 10x, 20x and 40× objectives (Nikon). Percentage of necrotic area was quantified in six fields per tissue sample from each mouse, where hepatocytes are the predominant cell type, using ImageJ software (NIH).

2.13. TUNEL staining

For cell death detection, paraffin-embedded liver biopsy sections were stained using the ApopTag Peroxidase *In Situ* Apoptosis detection Kit (S7100, Millipore by Merk, Darmstadt, Germany) according to the manual instructions. Images were taken using an optical microscope Nikon Model Eclipse E400 (Nikon) equipped with a plan Apocromatic 10x, 20x and 40× objectives (Nikon). The number of pyknotic nuclei and the total number of cells per 20x field were counted manually. Five representative fields per tissue sample from each mouse were scored, and reported as percentage of pyknotic nuclei (%).

2.14. 4-HNE detection by immunohistochemistry

Liver tissue sections were deparaffinized and rehydrated. Antigen retrieval was performed using HIER method: samples were boiled for 15 min in 10 mM sodium citrate pH 6.0. Sections were blocked prior to immunostaining with anti-4-HNE antibody 1:200 (ab46545, Abcam plc, Cambridge, UK) overnight. After incubation with secondary antibody, DAB detection system (EnVision ™ Flex Mini Kit, High pH (Link) Agilent, Santa Clara, CA, USA) was used for visualization according to the manufacturer's instructions. For histological assessment, six representative images were taken per section using a Nikon Eclipse E400 optical microscope (Nikon) equipped with a plan Apocromatic 10x, 20x and 40× objectives (Nikon). Intensity of 4-HNE stain was quantified using ImageJ software (NIH) and reported as the average value in arbitrary units (a.u.).

2.15. GSH levels determination

GSH content was quantitated by Hissin and Hilf fluorimetric assay, as

described elsewhere [36]. Protein liver homogenates were precipitated with 5% trichloroacetic acid and then centrifuged for 30 min at 10.000 g. The method is based on the reaction of GSH with *o*-phthalaldehyde (OPT) at pH 8.0 and fluorescence was measured at an excitation wavelength of 340 nm and an emission wavelength of 460 nm in a microplate reader (Bio-Tek, Winooski, VT, USA). Sample results were referred to those of a standard curve of GSH (5 ng–1 μg) and represented as percentage of GSH content.

2.16. Statistical analysis

Statistical analysis was performed using Graphpad prism (Docmatics, Boston, MA, USA) and the IBM SPSS Statistics 21.0 (SPSS Inc., IBM, Chicago, IL, USA) software. Quantitative variables are expressed as measures of central tendency (mean) and dispersion (standard error of mean; SEM). Data between groups were compared with Student's *t*-test for variables following a normal distribution and Mann-Whitney *U* test for continuous variables following a non-parametric distribution. For multiple comparison between groups, two-way ANOVA was performed. p value < 0.05 considered as statistically significant.

3. Results

3.1. Effects of pharmacological inhibition of BMP type I receptors in APAP-induced toxicity in hepatocytes

In order to explore the role of BMP signalling in APAP-induced ALF, we used several pharmacological inhibitors which present different selectivity for each receptor as shown in Table 1. Huh7 cells were treated with 10 μM DMH2 to selectively inhibit signalling through ALK3, 150 nM ML347 for ALK2 inhibition, and 500 nM LDN-193189 (LDN) to achieve inhibition of both receptors prior to stimulation with 20 mM APAP for 16 h. After exposure to these inhibitors, we only observed a modulation in ALK receptors expression in cells treated with DMH2: a decrease in *ALK3* mRNA and an up-regulation of *ALK2* (Fig. 1A). Moreover, lower phosphorylation of Smad 1/5/8 was observed for all of the inhibitors evidencing an efficient blockade of the signalling pathway (Fig. 1B). In addition, we quantified the expression of well-known BMP signalling target genes *ID1* and *HAMP* (genes which codifies for DNA binding protein inhibitor ID1 and hepcidin, respectively). As depicted in Fig. 1C and D, expression of *HAMP* was reduced in those cells where ALK2 was inhibited (LDN and ML347), while *ID1* mRNA expression was more significantly decreased in cells treated with those compounds inhibiting ALK3 (LDN and DMH2). Given that *HAMP* expression seems to be more influenced by signalling through ALK2 while *ID1* by signalling through ALK3, we used these two target genes to further validate the activation of these receptors in our cellular system. Notably, inhibition of ALK3 accomplished by DMH2 treatment granted higher cell viability after APAP exposure, and this protection was not achieved by using any of the other tested compounds (Fig. 1E).

Next, we evaluated if these results were recapitulated in primary mouse hepatocytes. For this purpose, cells were treated with 5 and 10 μM DMH2 in order to inhibit ALK3 signalling, prior to 10 mM APAP exposure. The results obtained showed higher viability after DMH2 treatment, compared to non-pre-treated hepatocytes (Fig. 1F). Since similar effect of DMH2 in primary hepatocytes and in the human hepatoma cell line Huh7 was found, we used Huh7 cells for further experiments.

As shown in Fig. 2A, higher cell survival was observed in those cells pre-treated with DMH2 compared to their corresponding controls. To deepen into this finding, we performed assays of cytotoxicity and apoptosis. We observed reduced APAP-induced toxicity, reflected in less release of lactate dehydrogenase (LDH) (Fig. 2B), as well as in decreased processing of caspase 3 (Fig. 2C), a marker of apoptosis, in APAP-exposed Huh7 cells pre-treated with DMH2 compared to Huh7 cells pre-treated with DMSO. In addition, it is well known that an antioxidant response is triggered in order to avoid APAP-induced oxidative stress [37]. Thus, *HMOX1* (hemoxygenase 1 –HO1- codifying gene), *GSTM3* (glutathione *S*-transferase Mu 3 codifying gene) and *SOD2* (superoxide dismutase 2 codifying gene) mRNA levels were measured as indicators of the activation of this antioxidant response. As expected, an induction of *HMOX1, GSTM3* and *SOD2* expression was observed after treatment with APAP; however, no increase of these antioxidant genes was detected in DMH2 pre-treated cells (Fig. 2D). Moreover, APAP-stimulated Huh7 cells pre-treated with DMH2 showed lower phosphorylation of the stress kinases JNK and P38 after APAP treatment (Fig. 2E).

In order to check whether these effects are due to the selective inhibition of ALK3, we explored the effect of LDN pre-treatment, which inhibits both ALK3 and ALK2 receptors, in Huh7 cells treated with APAP. The obtained results showed that the inhibition of both receptors neither reduced the APAP-mediated apoptotic effect (Fig. S1A) nor exerted any effect on the antioxidant system (Fig. S1B).

3.2. Silencing of BMP type I receptor ALK3 but not ALK2 protects against APAP-induced hepatotoxicity

To further corroborate the implication of BMP type I receptors ALK2 and ALK3 in APAP-induced acute liver damage, we performed a short hairpin knock-down of BMP type I receptors ALK2 and ALK3 in the hepatoma cell line Huh7. For this purpose, cells were infected with scrambled (ShControl), or ALK2 or ALK3 shRNA (ShALK2 or ShALK3, respectively) lentiviral particles. Efficiency of gene silencing was evaluated by measuring *ALK2* and *ALK3* mRNA and protein levels, obtaining a significant reduction of both receptors expression (Fig. 3A and B). Curiously, we found that ALK3 expression increased due to *ALK2* silencing, and ALK2 expression also was elevated in ShALK3 cells respect to the ShControls, similar to the modulation observed after DMH2 treatment (Fig. 3A and B). We also observed lower phosphorylation of Smad 1/5/8 in silenced cells (Fig. 3B), in parallel with a modulated expression of the target genes *ID1* and *HAMP*. As observed in the previous cellular model, *HAMP* expression decreased in ALK2-silenced cells while it increased in cells with a mild over-expression of ALK2 (ShALK3 cells); on the contrary, *ID1* expression was reduced after silencing of ALK3 and it was elevated in cells with a mild over-expression of ALK3 (ShALK2 cells) (Fig. 3C and D). Once established the silenced cell lines, they were treated with APAP and cellular viability was assessed, showing an increased cell survival in ShALK3 cells after APAP insult compared to ShControl. This effect was not observed in the ShALK2 cell line (Fig. 3E).

Moreover, we detected a significantly lower release of LDH as well as a lesser amount of the cleaved fragment of caspase 3 in ShALK3 cells treated with APAP compared to control cells (Fig. 4A and B, respectively). Furthermore, we used DHE probe to measure reactive oxygen species (ROS) production in these cells during the 2 h after APAP stimulation and we found that APAP-induced ROS was almost not observed in cells with silenced ALK3 (Fig. 4C). Interestingly, higher expression of the antioxidant genes *HMOX1, GSTM3* and *SOD2* at baseline and lower increase in the expression of these genes after APAP treatment was observed in ShALK3 cells compared to ShControl cells (Fig. 4D). Finally, lower levels of pJNK and pP38 were found in ALK3-silenced cells compared to control cells (Fig. 4E).

3.3. ALK2 over-expression displays an antiapoptotic effect against APAP insult

As stated above, *ALK2* mRNA expression was significantly increased in the stable cell line ShALK3 as well as in DMH2 pre-treated cells, possibly by a compensatory mechanism against the absence of ALK3 activation. In order to explore the implication of increased *ALK2* expression in ALK3-silenced cells, we infected Huh7 cells with lentiviral particles to generate a stable cell line over-expressing ALK2 (LV ALK2

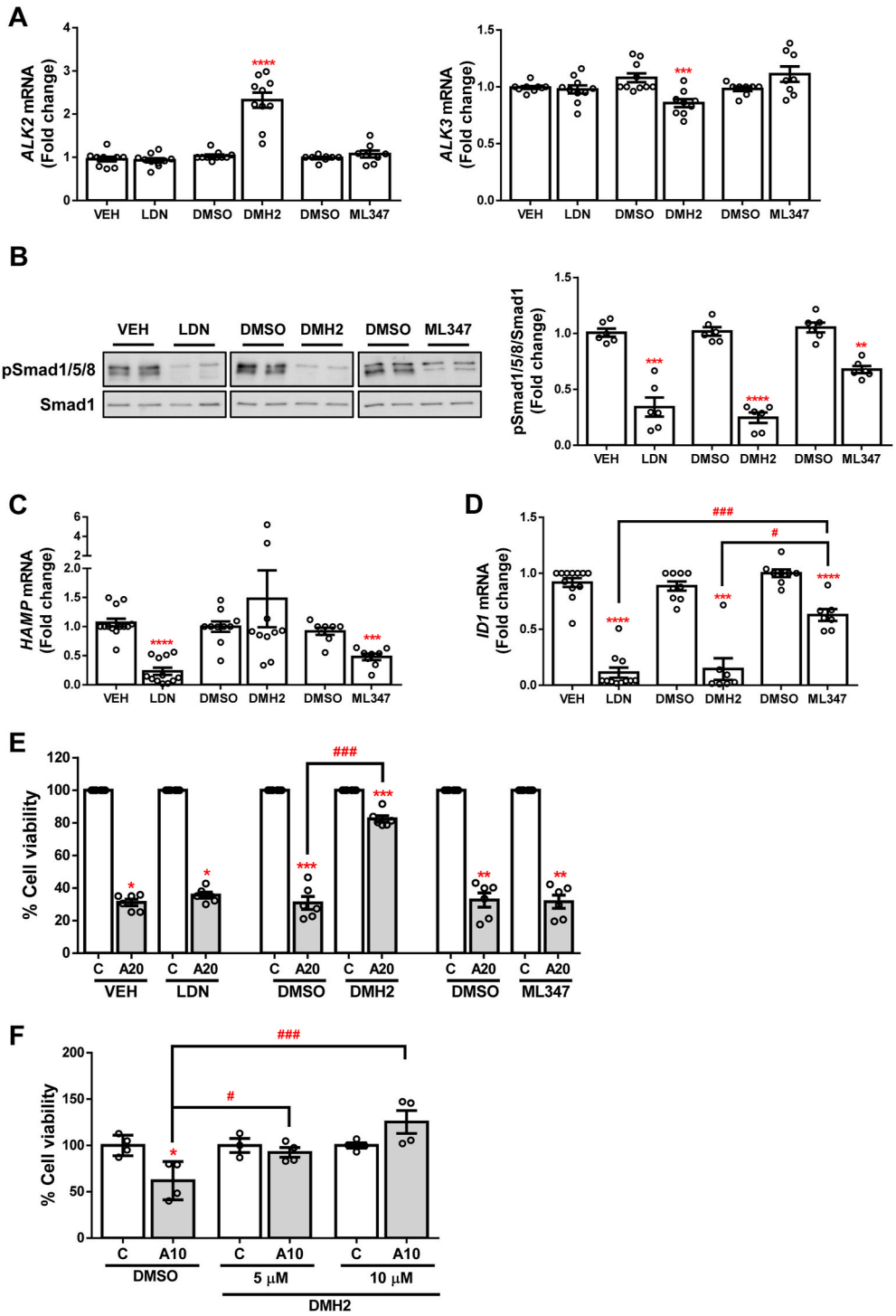

Fig. 1. Pharmacological inhibition of BMP type I receptors ALK2 and ALK3. A. mRNA levels of *ALK2* and *ALK3* determined by RT-qPCR and normalized to *36B4* gene expression. Data are expressed as fold increase relative to control condition (vehicle; VEH or DMSO, 1) and presented as mean ± SEM. **B.** Representative blots with the indicated antibodies and the corresponding quantification. Data are expressed as fold change relative to the control condition (vehicle; VEH or DMSO, 1) and presented as mean ± SEM. **C – D.** *HAMP* and *ID1* mRNA levels determined by RT-qPCR and normalized to *36B4* gene expression. Data are expressed as fold increase relative to the control condition (vehicle; VEH or DMSO, 1) and presented as mean ± SEM. Experimental conditions: Huh7 treated with the inhibitors LDN-193189 (LDN) (500 nM), DMH2 (10 μM) or ML347 (150 nM) for 16 h ($n \geq 3$ independent experiments). $^{**}p < 0.01$, $^{***}p < 0.005$ and $^{****}p < 0.0001$, LDN *vs.* VEH, or DMH2 or ML347 *vs.* DMSO; $^{\#}p < 0.05$ and $^{\#\#\#}p < 0.005$, ML347 *vs.* DMH2 or LDN. **E – F.** Cell viability determined by crystal violet staining. Data are represented as percentage relative to the control group (vehicle; VEH or DMSO, 100%) and presented as mean ± SEM. Experimental conditions: (E) Huh7 treated with the inhibitors LDN-193189 (LDN) (500 nM), DMH2 (10 μM) or ML347 (150 nM) 1 h prior to APAP (20 mM, A20) stimulation for 16 h ($n \geq 3$ independent experiments). (F) Primary mouse hepatocytes treated with the inhibitor DMH2 (5 or 10 μM) 1 h prior to APAP (10 mM, A10) stimulation for 16 h ($n = 2$ independent experiments performed by duplicate). $^{*}p < 0.05$, $^{**}p < 0.01$ and $^{***}p < 0.005$, A10 or A20 *vs.* C; $^{\#}p < 0.05$ and $^{\#\#\#}p < 0.005$, A10/20-DMH2 *vs.* A10/20-DMSO. (For interpretation of the references to color in this figure legend, the reader is referred to the Web version of this article.)

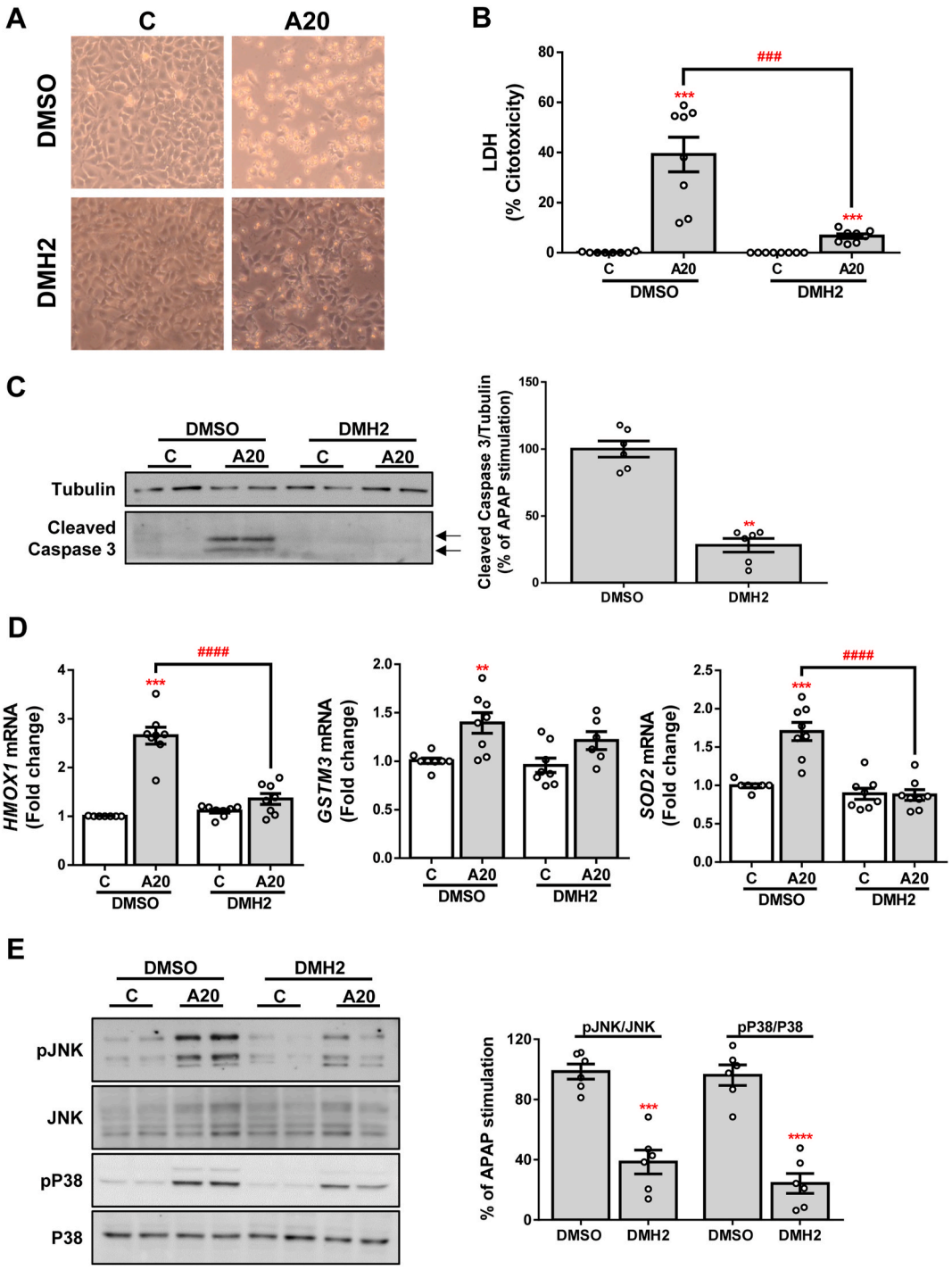

Fig. 2. Pharmacological inhibition of ALK3 with DMH2 protects against APAP-induced hepatotoxicity. A. Representative phase-contrast images of Huh7 cells treated with the inhibitor DMH2 (10 μM) 1 h prior to APAP (20 mM, A20) stimulation for 16 h. **B.** Cytotoxicity determined by lactate dehydrogenase (LDH) release. Data are presented as percentage relative to the positive control (100%) and presented as mean ± SEM. **C.** Representative blots with the indicated antibodies and the corresponding quantification. Data are expressed as percentage relative to the control group (DMSO, 100%) and presented as mean ± SEM. **D.** mRNA levels of *HMOX1, GSTM3* and *SOD2* determined by RT-qPCR and normalized to *36B4* gene expression. Data are expressed as fold increase relative to the control condition (C-DMSO, 1) and presented as mean ± SEM. **E.** Representative blots with the indicated antibodies and the corresponding quantification. Data are expressed as percentage relative to the control group (DMSO, 100%) and presented as mean ± SEM. Experimental conditions: Huh7 treated with the inhibitor DMH2 (10 μM) 1 h prior to APAP (20 mM, A20) stimulation for 6 (E) or 16 (A–D) hours (n ≥ 3 independent experiments). **p < 0.01, ***p < 0.005 and ****p < 0.0001, A20 *vs.* C, or DMH2 *vs.* DMSO; $^{###}$p < 0.005 and $^{####}$p < 0.0001, A20-DMH2 *vs.* A20-DMSO.

OE) and its respective control (LV Control). The over-expression of ALK2 was evaluated by measuring mRNA levels of this receptor which showed a 3-fold increased expression (Fig. 5A). Likewise, the expression of its target gene *HAMP* was significantly increased, while mRNA levels of *ALK3* and *ID1* were not modulated (Fig. 5B). After stimulation with APAP, LV ALK2 OE cells did not show higher cell viability (Fig. 5C). However, a strong inhibition of the cleavage of caspase 3 was observed, indicating that ALK2 over-expression displays an antiapoptotic effect (Fig. 5D). On the contrary, mRNA expression of *HMOX1* was similar in both groups (Fig. 5E) and no differences in phosphorylation of the

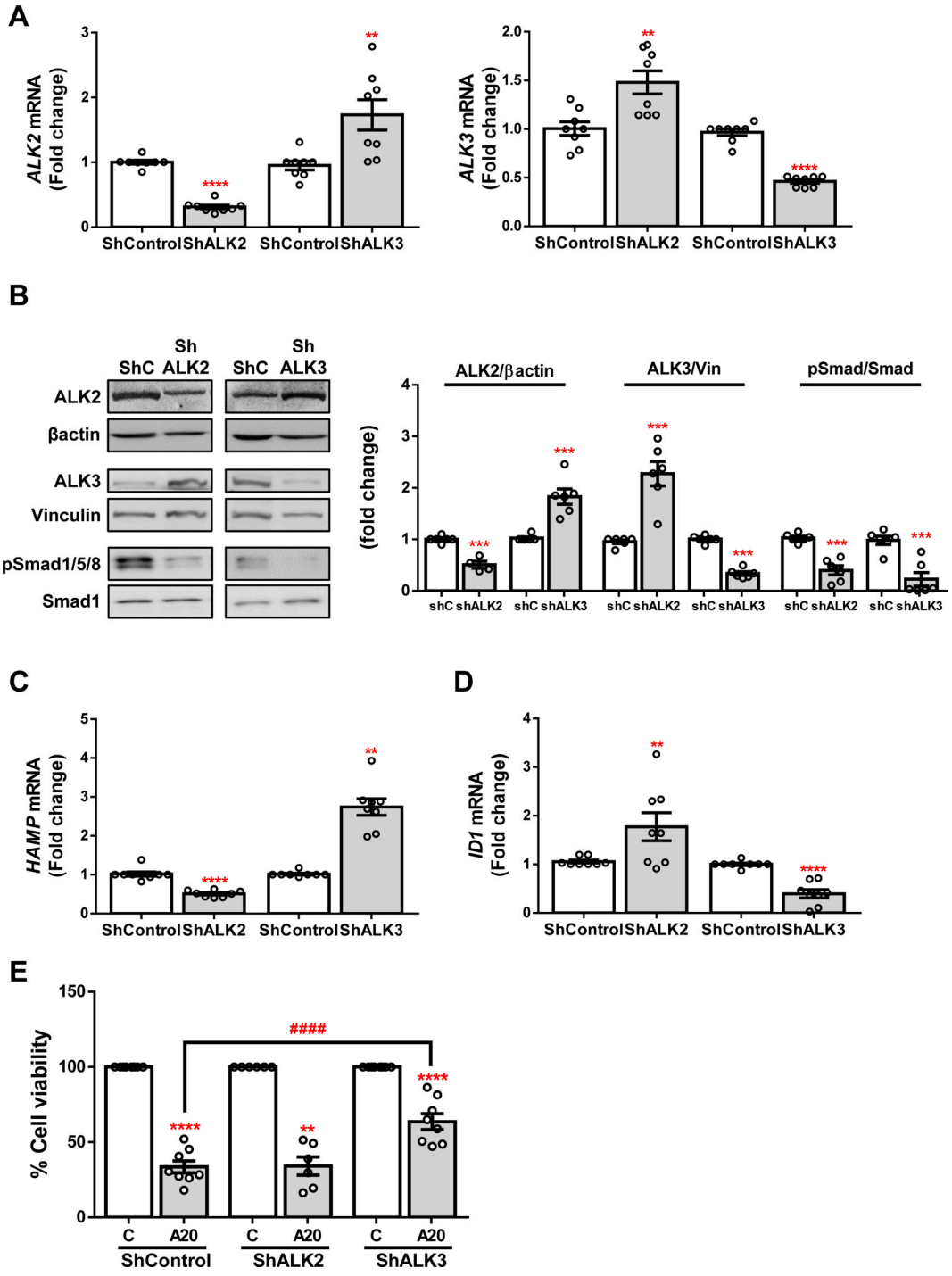

Fig. 3. Effect of silencing of BMP type I receptors ALK3 and ALK2 on cellular viability on Huh7 human hepatocytes. A. mRNA levels of *ALK2* (left) and *ALK3* (right) determined by RT-qPCR and normalized to *36B4* gene expression. **B.** Representative blots with the indicated antibodies and the corresponding quantification. Data are expressed as fold increase relative to the control condition (ShControl, 1) and presented as mean ± SEM. **C - D.** mRNA levels of *HAMP* and *ID1*, respectively, determined by RT-qPCR and normalized to *36B4* gene expression. Data are expressed as fold increase relative to the control condition (ShControl, 1) and presented as mean ± SEM. Experimental conditions: Huh7 silenced stable lines ShALK2 and ShALK3 and their control ShControl (ShC) treated (n ≥ 3 independent experiments). **p < 0.01, ***p < 0.005 and ****p < 0.0001, ShALK2 or ShALK3 *vs.* ShC. **E.** Cell viability determined by crystal violet staining. Data are represented as percentage relative to control group (C, 100%) and presented as mean ± SEM. Experimental conditions: Huh7 silenced stable lines ShALK2 and ShALK3 and their control ShControl (ShC) treated with APAP (20 mM, A20) for 16 h (n ≥ 3 independent experiments). **p < 0.01 and ****p < 0.0001, A20 *vs.* C; $^{\#\#\#\#}$p < 0.0001, A20-ShALK3 *vs.* A20-ShC. (For interpretation of the references to color in this figure legend, the reader is referred to the Web version of this article.)

kinases JNK and P38 after APAP treatment were found (Fig. 5F).

3.4. DMH2 inhibitor protects against APAP-induced hepatotoxicity in vivo

In an attempt to explore whether the effects observed after ALK3 inhibition in APAP-induced toxicity in a cellular system could be

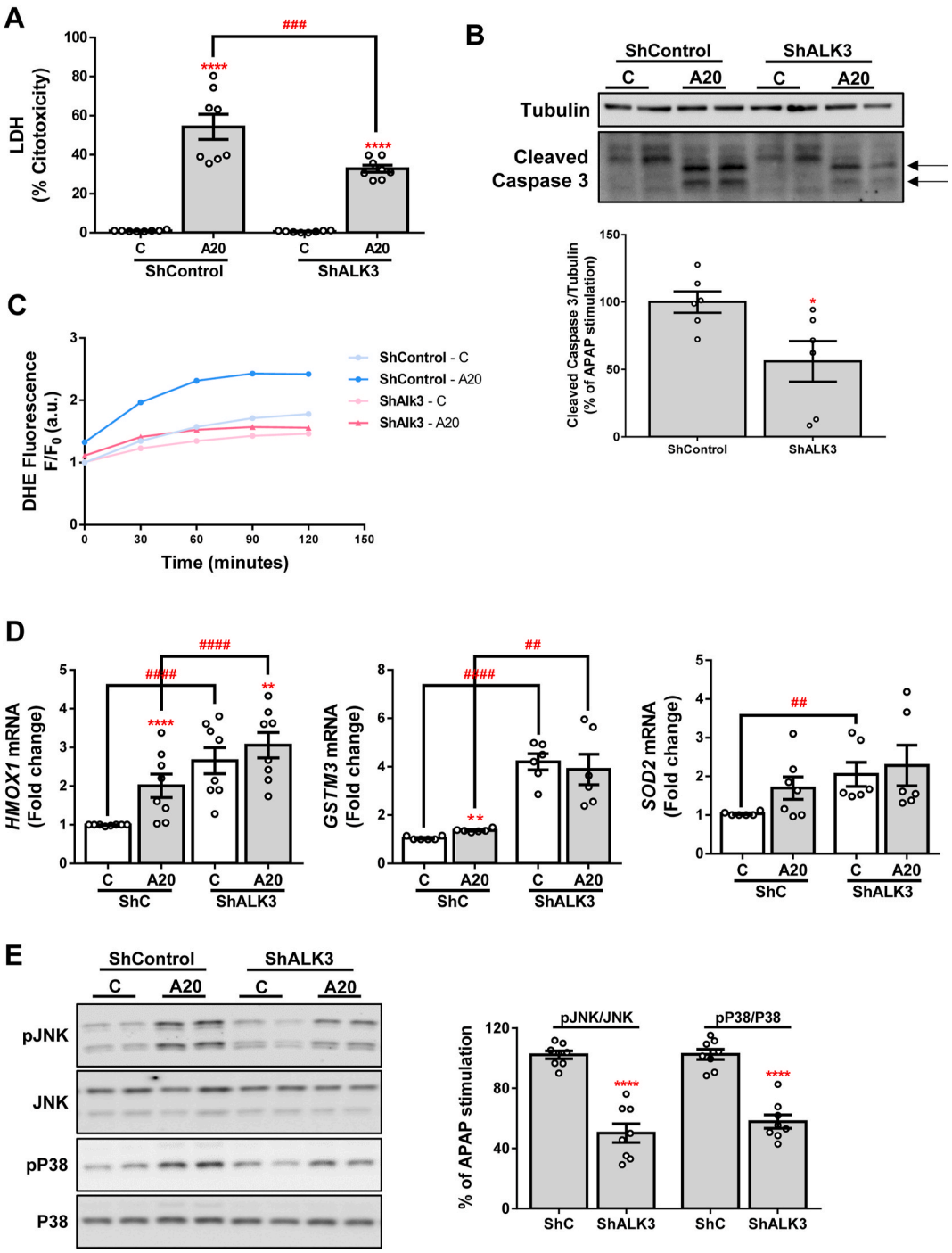

Fig. 4. Silencing of *ALK3* protects against APAP-induced cell toxicity. A. Cytotoxicity determined by lactate dehydrogenase (LDH) release. Data are presented as percentage relative to the positive control (100%). **B.** Representative blots with the indicated antibodies and the corresponding quantification. Data are expressed as percentage relative to the control group (ShControl, 100%) and presented as mean ± SEM. **C.** ROS production detected with DHE probe represented as DHE fluorescence F/F_0 (a.u.) through exposure to APAP during 2 h. **D.** mRNA levels of *HMOX1, GSTM3* and *SOD2* determined by RT-qPCR and normalized to *36B4* gene expression. Data are expressed as fold increase relative to the control condition (ShControl 1) and presented as mean ± SEM. **E.** Representative blots with the indicated antibodies and the corresponding quantifications. Data are expressed as percentage relative to control group (ShControl, 100%) and presented as mean ± SEM. Experimental conditions: Huh7 silenced stable line ShALK3 and its control ShControl (ShC) treated with APAP 20 mM (A20) for 2 (C), 6 (E) or 16 (A, B, D) hours (n ≥ 3 independent experiments). *p < 0.05, **p < 0.01 and ****p < 0.0001, A20 *vs.* C, or ShALK3 *vs.* ShC; $^{\#}$p < 0.05, $^{\#\#\#}$p < 0.005 and $^{\#\#\#\#}$p < 0.001, C-ShALK3 *vs.* C-ShC or A20-ShALK3 *vs.* A20-ShC.

reproduced *in vivo,* we performed an experimental model of APAP-induced ALF in mice. Since we wanted to evaluate the potential effects of the administration of DMH2 on liver damage after APAP overdose, we firstly checked that DMH2 also increased cell viability after APAP treatment *in vitro* when it was added to hepatocytes 1 h after APAP (Fig. S4). Then, mice were i. p. injected with vehicle (DMSO) or APAP (500 mg/kg) and, 1 h later, DMH2 or the corresponding amount of DMSO was administrated in a single dose of 3 mg/kg (Fig. 6A). In order to assess the effect of DMH2 on APAP-induced liver damage, we quantified the percentage of injured areas in the liver tissue of these animals.

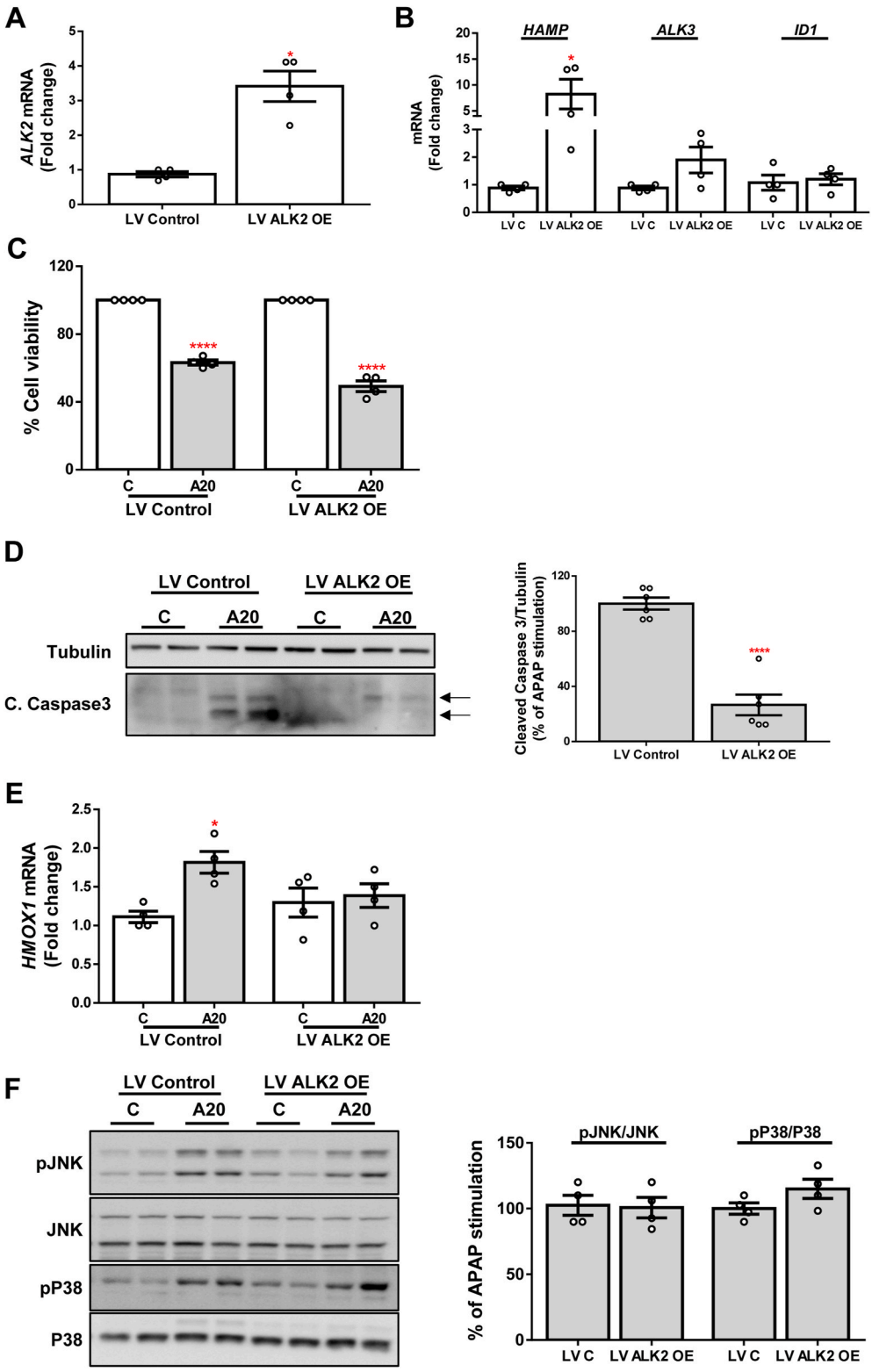

Fig. 5. Antiapoptotic effect of *ALK2* over-expression. A - B. mRNA levels of *ALK2, HAMP, ALK3* and *ID1* determined by RT-qPCR and normalized to *36B4* gene expression. Data are expressed as fold increase relative to control condition (LV Control, 1) and presented as mean ± SEM. **C.** Cell viability determined by crystal violet staining. Data are represented as percentage relative to control group (C, 100%). **D.** Representative blots with the indicated antibodies and the corresponding quantification. Data are expressed as percentage relative to control group (LV Control, 100%). **E.** mRNA levels of *HMOX1* determined by RT-qPCR and normalized to *36B4* gene expression. Data are expressed as fold increase relative to control condition (C-LV Control, 1) and presented as mean ± SEM. **F.** Representative blots with the indicated antibodies and the corresponding quantifications. Data are expressed as percentage relative to control group (LV Control, 100%) and presented as mean ± SEM. Experimental conditions: Huh7 cell line over-expressing ALK2 (LV ALK2 OE) and their control (LV Control, LV C) treated with APAP (20 mM, A20) for 6 (F) or 16 (A–E) hours ($n \geq 3$ independent experiments). *$p < 0.05$ and ****$p < 0.0001$, LV ALK2 OE *vs.* LV C, or A20 *vs.* C. (For interpretation of the references to color in this figure legend, the reader is referred to the Web version of this article.)

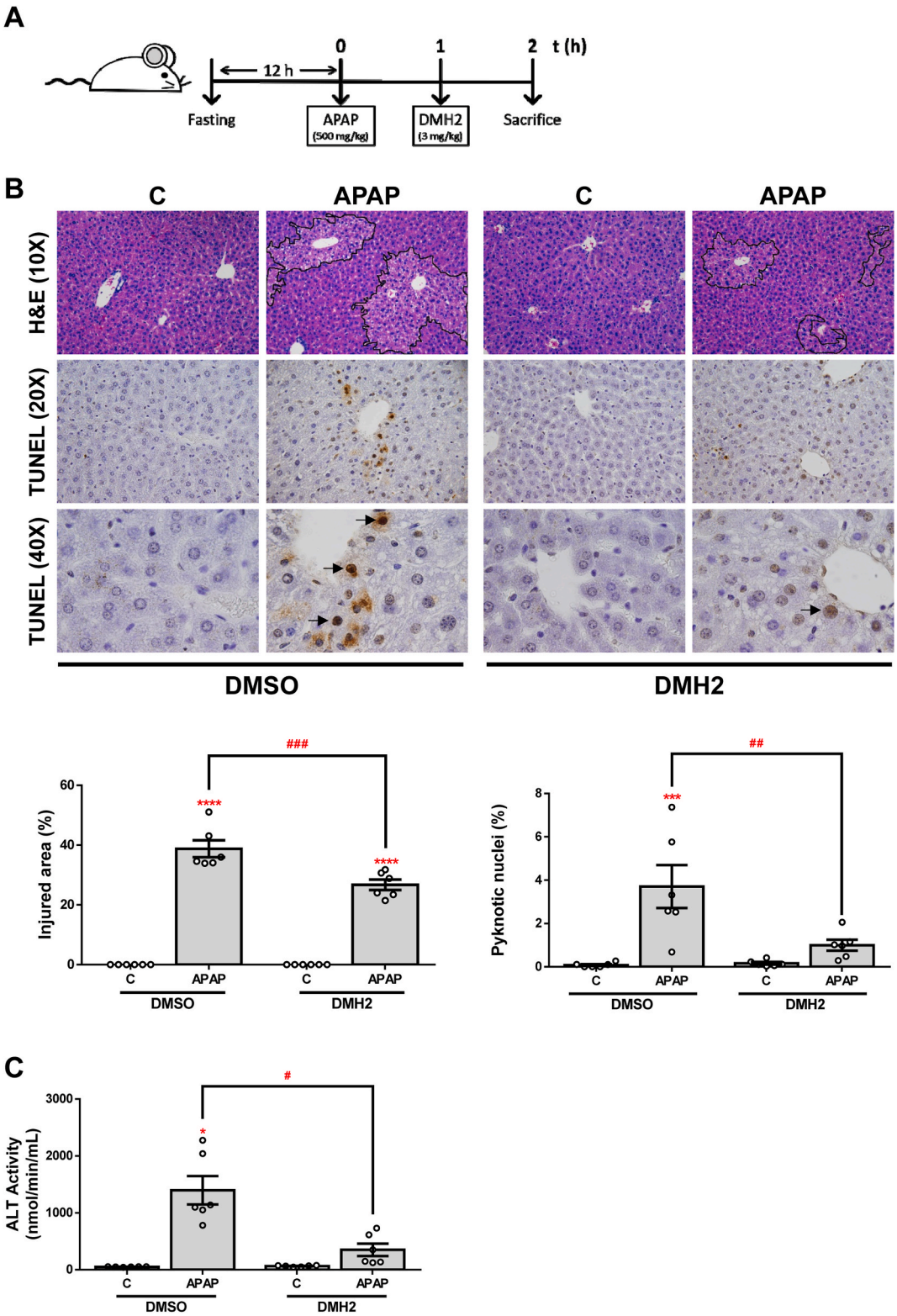

Fig. 6. The ALK3 inhibitor DMH2 protects against liver damage in an animal model of APAP-induced acute liver failure. A. *Experimental conditions*: Mice i. p. injected with vehicle (DMSO) or APAP (500 mg/kg), and 1 h later treated with DMH2 or the corresponding amount of DMSO in a single dose of 3 mg/kg. Animals were sacrificed 2 h after APAP administration (n = 6 animals per group). **B.** Representative 10X images of H&E, and 20X and 40X images of TUNEL staining and the corresponding quantifications. Data are expressed as percentage of injured area or pyknotic nuclei, respectively and presented as mean ± SEM. **C.** ALT activity determination in serum samples presented as mean ± SEM. *p < 0.05, ***p < 0.005 and ****p < 0.0001, APAP *vs.* C; $^{\#}$p < 0.05, $^{\#\#}$p < 0.01 and $^{\#\#\#}$p < 0.005, APAP-DMH2 *vs.* APAP-DMSO.

Notably, a significant reduction of APAP-induced hepatocyte damage was observed only in those mice treated with DMH2 after APAP challenge. Likewise, TUNEL staining revealed less presence of pyknotic nuclei in the livers from animals with DMH2 treatment (Fig. 6B). In addition, serum ALT levels after APAP-induced liver injury were significantly lower in mice treated with DMH2 than in those receiving with vehicle (Fig. 6C).

As previously mentioned, one of the main features of APAP-induced liver injury is the production of ROS and the triggering of antioxidant mechanisms in response to oxidative stress. In order to assess the effects of DMH2 treatment on APAP-mediated oxidative stress, we measured the hepatic expression of several antioxidant genes. As expected, a marked increase of *Hmox1, Gstm3, Sod2, Cat* (catalase codifying gene) and *Gpx1* (glutathione peroxidase 1 codifying gene) expression was observed in liver samples from mice exposed to an APAP overdose, but this increase was milder or not observed in the presence of DMH2 (Fig. 7A). According to these data, treatment with DMH2 also significantly reduced APAP-induced GSH depletion (Fig. 7B). To further validate this finding, we quantified the hepatic expression of 4-HNE, a secondary product of lipid peroxidation, by immunohistochemistry. Notably, the expression of 4-HNE was significantly lower in the livers from animals treated with DMH2 than in those treated with vehicle (Fig. 7C). Finally, lower levels of pJNK were found in DMH2-treated mice (Fig. 7D).

For the evaluation of later time points, we have analysed livers from mice that have been sacrificed 6 h after DMH2 post-APAP treatment (Fig. S2A). Although we found a protection from APAP hepatotoxicity (necrosis, apoptosis, ALT levels and lipid peroxidation), this effect was not statistically significant in all the parameters tested, likely due to an attenuation of the effect of DMH2 at longer time-periods (Figs. S2 and S3).

4. Discussion

ALF is characterized by a massive death of the hepatocytes. Therefore, the identification of novel protective mechanisms against hepatocyte damage might help in the development of new therapeutic approaches against ALF. This study identified a novel role of BMP signal transduction pathway in ALF, particularly in hepatotoxicity due to an APAP overdose.

BMPs signal through two types of serine/threonine receptors [14]: type I receptors (ALK receptors) and type II receptors (BMPRII, ACTRIIA and ACTRIIB). Type I receptors are expressed in the liver and include ALK2 and ALK3 [21] which activate downstream signalling via Smad1/5/8 phosphorylation [38,39]. Importantly, the transcription of the different BMP target genes depends on different factors such as the cellular type [14,21]. In our experiments in ALK-inhibited or silenced Huh7 cells, we observed that *ALK2* expression increased due to *ALK3* silencing, and *viceversa*. Moreover, we found that ALK2 plays a critical role in *HAMP* expression since by selectively targeting ALK2, but not ALK3, hepcidin gene expression was effectively modulated while, on the contrary, specific regulation of ALK3, but not ALK2, markedly controlled *ID1* expression. Consequently, we used these two target genes to further corroborate the activation of these two ALK receptors in hepatocytes.

With the purpose of clarifying the role of ALK2 and ALK3, we tested known pharmacologic agents targeting BMP signalling and explored their effect on APAP-induced hepatic toxicity. The *in vitro* experiments showed that only DMH2, which selectively inhibits BMP signalling through ALK3, protects against APAP-induced hepatotoxicity in both the hepatoma cell line Huh7 and in primary mouse hepatocytes. Indeed, ALK3 inhibition by DMH2 treatment reduced both necrosis, assessed by LDH release, and apoptosis, measured by the cleavage of caspase 3, following APAP overdose compared to non-treated cells. Also, ROS-mediated JNK and P38 MAPK phosphorylation was reduced, as well as the induction of antioxidant gene expression, in DMH2 treated cells compared to control cells upon APAP challenge. Indeed, we would expect that LDN might have exerted the same effects as it inhibits both receptors, but it did not. This could be due to the concomitant mild over-expression of *ALK2* that is found upon ALK3 inhibition that is likely necessary for the protective effects.

In order to corroborate the data observed in DMH2 treated cells, we silenced *ALK2* and *ALK3* in Huh7 cells. We found that ALK3, but not ALK2, inhibition protects against APAP-induced hepatotoxicity, reproducing the effects of DMH2 treatment, demonstrating an important role for this BMP type I receptor in APAP-induced liver injury. Also, ROS generation was ameliorated, while a constitutively increased expression of the antioxidant genes *HMOX1*, *GSTM3* and *SOD2* was found in *ALK3*-silenced hepatocytes, possibly reflecting that these cells present a more active antioxidant defence against oxidative stressors such as APAP. To further clarify whether the protective effects observed were not derived from the concomitant upregulation of *ALK2* expression observed in ShALK3 cells, we generated a stable cell line over-expressing *ALK2*. The over-expression of ALK2 receptor in hepatocytes neither improved cell viability nor modified the response to APAP-induced oxidative stress; however, hepatocytes over-expressing *ALK2* showed a higher anti-apoptotic capacity. Previous studies have reported an antiapoptotic effect of BMP signalling through the canonical pathway by inducing the expression of X-linked inhibitor of apoptosis protein (XIAP), a potent caspase 3 inhibitor [40]. Also, it has been observed that DMH2 treatment in lung cancer-derived cells increased cellular death by reducing XIAP expression [33]. Even though these results oppose to those showed in this study, in our cellular model DMH2 seemed to specifically inhibit ALK3-mediated signalling while induced that mediated by ALK2, which in turn could be responsible of the apoptotic effect observed in lung cells. This might also explain the lack of effect of the ALK2 and ALK3 inhibitor LDN in lowering caspase 3 processing, while over-expression of ALK2 does confer this antiapoptotic effect. Further investigations are needed to fully elucidate the molecular mechanisms underlying the novel roles of ALK receptors in mediating antioxidant defence and apoptosis in hepatocytes which have been reported herein for the first time.

The important role of BMP signalling in the pathogenesis of APAP-induced liver injury indicates that the BMP signal transduction pathway may be a successful target for future approaches to the treatment and/or co-treatment of this disease. Indeed, although APAP hepatotoxicity remains the leading cause of ALF, treatment options are limited. Nowadays, NAC is the first line treatment for patients with APAP-induced DILI; however, it has a narrow therapeutic window [11]. In this regard, since pharmacologic antagonism of BMPs with different inhibitors is possible and tolerable *in vivo*, we designed an experimental model in mice treated or not with DMH2 after APAP-induced ALF. Interestingly, we observed that only livers from mice treated with DMH2 were protected from APAP-induced damage, suggesting for the first time that ALK3 might be a novel therapeutic target for ALF. BMP signalling pathway has been implicated in the pathophysiology of chronic liver diseases such as NAFLD and hepatic fibrosis/HCC [41,42], but its role in ALF has not previously been established. In the present study, we provide convincing experimental evidence on the efficacy of the pharmacological inhibition of BMP signalling by using DMH2 markedly to attenuate hepatocyte damage by reducing the levels of serum transaminases, and preventing oxidative stress induced by an overdose of APAP in mice.

Taking all into account, this study demonstrated that the inhibition of ALK3 protects against APAP-induced hepatotoxicity, providing new mechanistic evidence on the role of BMP signalling in the pathogenesis of liver injury mediated by APAP. These striking experimental findings open up a novel therapeutic approach for patients with ALF due to APAP overdose and, therefore, clinical studies to assess safety and efficacy of targeting BMP signalling in patients with this life-threatening disorder are warranted.

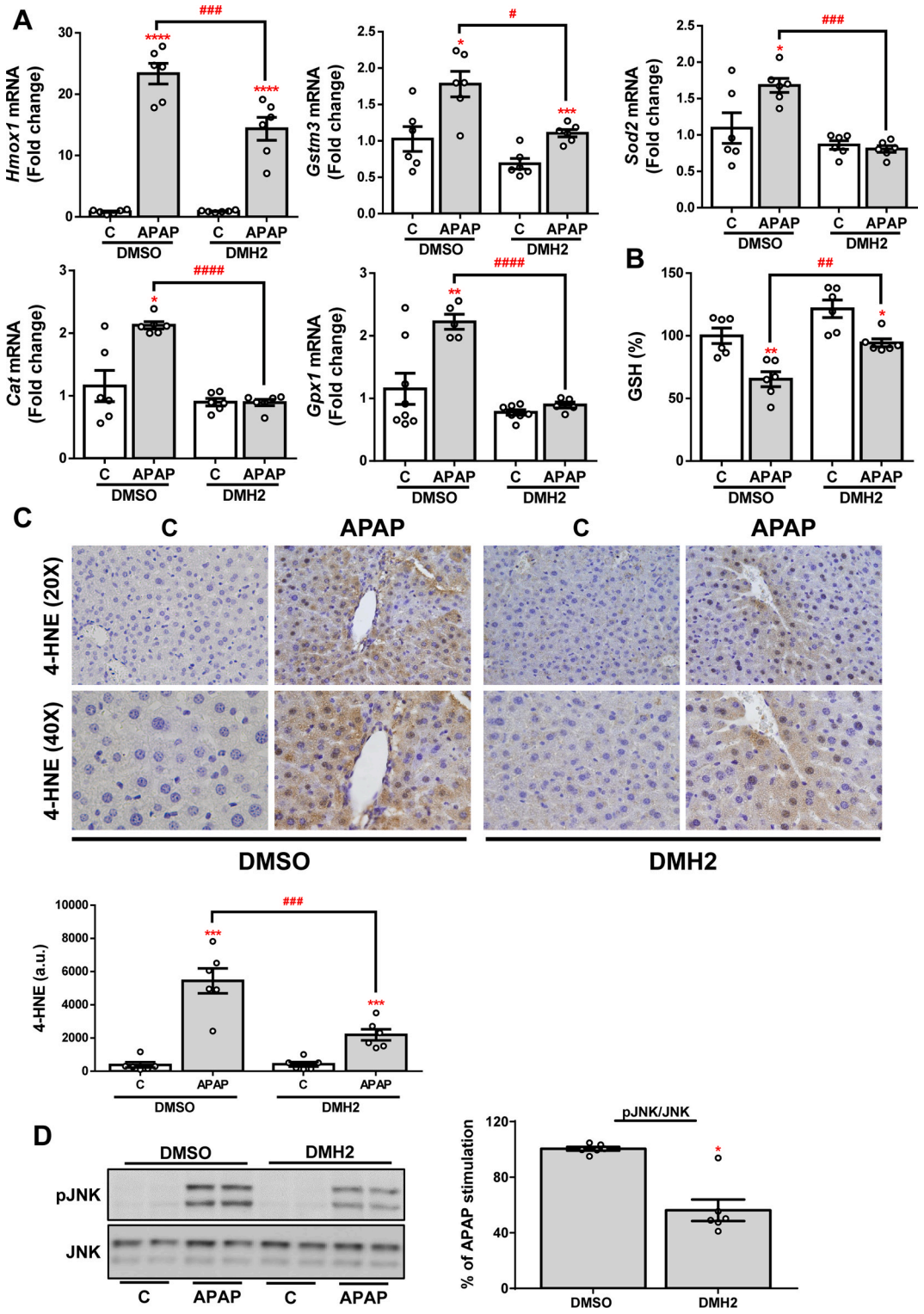

Fig. 7. DMH2 ameliorates oxidative stress in an animal model of APAP- induced acute liver failure. A. mRNA levels of *Hmox1, Gstm3, Sod2, Cat* and *Gpx1* determined by RT-qPCR and normalized to *36b4* gene expression. Data are expressed as fold increase relative to the control condition (C-DMSO, 1) and presented as mean ± SEM. **B.** GSH levels. Data are expressed as percentage relative to the control group (C-DMSO, 100%) and presented as mean ± SEM. **C.** Representative 20X and 40X images of 4-HNE IHC in liver sections and the corresponding quantification. Data are presented as mean ± SEM and expressed as arbitrary units (a.u.). **D.** Representative blots with the indicated antibodies and the corresponding quantification. Data are presented as mean ± SEM and expressed as percentage relative to control group (C-DMSO, 100%). *Experimental conditions*: Mice i. p. Injected with vehicle (DMSO) or APAP (500 mg/kg), and 1 h later treated with DMH2 or the corresponding amount of DMSO in a single dose of 3 mg/kg. Animals were sacrificed 2 h after APAP administration (n = 6 animals per group). *p < 0.05, **p < 0.01, ***p < 0.005 and ****p < 0.0001, APAP *vs.* C; #p < 0.05, ##p < 0.01, ###p < 0.005 and ####p < 0.001, APAP-DMH2 *vs.* APAP-DMSO.

Funding

This study was supported by grants RTI2018-094203-B-I00 (to AMR), PID2020-11794RB-IOO (to FJC), PID2021-124688OB-I00 (to AMR) and PID2021-122766OB-100 (to AMV) and funded by MCIN/AEI/10.13039/501100011033 (Spain) and "ERDF A way of making Europe" by the European Union; the European Horizon's research and innovation programme HORIZON-HLTH-2022-STAYHLTH-02 under agreement No 101095679, funded by the European Union, and COST Action CA17112, supported by COST (European Cooperation in Science and Technology), to FJC, and contract CP19/00032, and grants PI16/00853 and PI19/00123 from Instituto de Salud Carlos III (ISCIII, Spain), partially funded by FEDER, and CIBERDEM (ISCIII, Spain) to AGR. FJC belongs to the validated Research Groups Ref. 970935 "Liver Pathophysiologÿ, 920631 "Lymphocyte immunobiologÿ, 920361 "Inmunogenética e inmunología de las mucosas" and IBL-6 (imas12-associated). CCF is supported by grant FPU18/03475 from the Ministerio de Universidades (Spain), partially funded by FEDER. PMB is supported by a research contracts (PEJD-2018-PRE/BMD-9500PEJ-2020-AI/BMD-19491) funded by Comunidad de Madrid (Spain). SCI is supported by a predoctoral contract (FI20-00296) from ISCIII/FEDER (Spain).

CRediT authorship contribution statement

Patricia Marañón: Data curation, Formal analysis, Investigation, Methodology, Software, Writing – original draft, Conceptualization, Writing – review & editing. **Esther Rey:** Data curation, Formal analysis, Methodology. **Stephania C. Isaza:** Data curation, Formal analysis, Methodology, Writing – review & editing. **Hanghang Wu:** Data curation. **Patricia Rada:** Data curation, Formal analysis. **Carmen Choya-Foces:** Methodology, Writing – review & editing. **Antonio Martínez-Ruiz:** Methodology, Writing – review & editing. **María Ángeles Martín:** Methodology, Writing – review & editing. **Sonia Ramos:** Methodology, Writing – review & editing. **Carmelo García-Monzón:** Writing – review & editing. **Francisco Javier Cubero:** Methodology, Writing – review & editing. **Ángela M. Valverde:** Methodology, Writing – review & editing. **Águeda González-Rodríguez:** Conceptualization, Formal analysis, Funding acquisition, Investigation, Methodology, Project administration, Resources, Software, Supervision, Validation, Visualization, Writing – original draft, Writing – review & editing.

Declaration of competing interest

None'.

Appendix A. Supplementary data

Supplementary data to this article can be found online at https://doi.org/10.1016/j.redox.2024.103088.

References

[1] W.M. Lee, R.H. Squires, S.L. Nyberg, E. Doo, J.H. Hoofnagle, Acute liver failure: summary of a workshop, Hepatology 47 (4) (2008) 1401–1415.
[2] W.M. Lee, Acetaminophen (APAP) hepatotoxicity-Isn't it time for APAP to go away? J. Hepatol. 67 (6) (2017) 1324–1331.
[3] M. Jóźwiak-Bebenista, J.Z. Nowak, Paracetamol: mechanism of action, applications and safety concern, Acta Pol. Pharm. 71 (1) (2014) 11–23.
[4] C. Pezzia, C. Sanders, S. Welch, A. Bowling, W.M. Lee, A.L.F.S. Group, Psychosocial and behavioral factors in acetaminophen-related acute liver failure and liver injury, J. Psychosom. Res. 101 (2017) 51–57.
[5] C. Bunchorntavakul, K.R. Reddy, Acetaminophen (APAP or N-Acetyl-p-Aminophenol) and acute liver failure, Clin. Liver Dis. 22 (2) (2018) 325–346.
[6] M. Yan, Y. Huo, S. Yin, H. Hu, Mechanisms of acetaminophen-induced liver injury and its implications for therapeutic interventions, Redox Biol. 17 (2018) 274–283.
[7] A. Ramachandran, H. Jaeschke, Acetaminophen toxicity: novel insights into mechanisms and future perspectives, Gene Expr. 18 (1) (2018) 19–30.
[8] K. Du, A. Ramachandran, H. Jaeschke, Oxidative stress during acetaminophen hepatotoxicity: sources, pathophysiological role and therapeutic potential, Redox Biol. 10 (2016) 148–156.
[9] A. Iorga, L. Dara, N. Kaplowitz, Drug-induced liver injury: cascade of events leading to cell death, apoptosis or necrosis, Int. J. Mol. Sci. 18 (5) (2017).
[10] D.G. Craig, A. Lee, P.C. Hayes, K.J. Simpson, Review article: the current management of acute liver failure, Aliment. Pharmacol. Ther. 31 (3) (2010) 345–358.
[11] StatPearls, Chapter: Acetaminophen Toxicity, Section: Treatment/Management (2022). https://www.ncbi.nlm.nih.gov/books/NBK441917/.
[12] G.F. Rushworth, I.L. Megson, Existing and potential therapeutic uses for N-acetylcysteine: the need for conversion to intracellular glutathione for antioxidant benefits, Pharmacol. Ther. 141 (2) (2014) 150–159.
[13] E.S. Fisher, S.C. Curry, Evaluation and treatment of acetaminophen toxicity, Adv. Pharmacol. 85 (2019) 263–272.
[14] T. Katagiri, T. Watabe, Bone morphogenetic proteins, Cold Spring Harbor Perspect. Biol. 8 (6) (2016).
[15] M.C. Gomez-Puerto, P.V. Iyengar, A. García de Vinuesa, P. Ten Dijke, G. Sanchez-Duffhues, Bone morphogenetic protein receptor signal transduction in human disease, J. Pathol. 247 (1) (2019) 9–20.
[16] A.C. Carreira, G.G. Alves, W.F. Zambuzzi, M.C. Sogayar, J.M. Granjeiro, Bone Morphogenetic Proteins: structure, biological function and therapeutic applications, Arch. Biochem. Biophys. 561 (2014) 64–73.
[17] T.D. Mueller, J. Nickel, Promiscuity and specificity in BMP receptor activation, FEBS Lett. 586 (14) (2012) 1846–1859.
[18] B. Bragdon, O. Moseychuk, S. Saldanha, D. King, J. Julian, A. Nohe, Bone morphogenetic proteins: a critical review, Cell. Signal. 23 (4) (2011) 609–620.
[19] S. Saremba, J. Nickel, A. Seher, A. Kotzsch, W. Sebald, T.D. Mueller, Type I receptor binding of bone morphogenetic protein 6 is dependent on N-glycosylation of the ligand, FEBS J. 275 (1) (2008) 172–183.
[20] G. Sanchez-Duffhues, E. Williams, M.J. Goumans, C.H. Heldin, P. Ten Dijke, Bone morphogenetic protein receptors: structure, function and targeting by selective small molecule kinase inhibitors, Bone 138 (2020) 115472.
[21] Y. Xia, J.L. Babitt, Y. Sidis, R.T. Chung, H.Y. Lin, Hemojuvelin regulates hepcidin expression via a selective subset of BMP ligands and receptors independently of neogenin, Blood 111 (10) (2008) 5195–5204.
[22] S. Canali, C.Y. Wang, K.B. Zumbrennen-Bullough, A. Bayer, J.L. Babitt, Bone morphogenetic protein 2 controls iron homeostasis in mice independent of Bmp 6, Am. J. Hematol. 92 (11) (2017) 1204–1213.
[23] D. Meynard, L. Kautz, V. Darnaud, F. Canonne-Hergaux, H. Coppin, M.P. Roth, Lack of the bone morphogenetic protein BMP6 induces massive iron overload, Nat. Genet. 41 (4) (2009) 478–481.
[24] R.P. van Swelm, C.M. Laarakkers, L. Blous, J.G. Peters, E.N. Blaney Davidson, P. M. van der Kraan, et al., Acute acetaminophen intoxication leads to hepatic iron loading by decreased hepcidin synthesis, Toxicol. Sci. 129 (1) (2012) 225–233.
[25] T.B. Chaston, P. Matak, K. Pourvali, S.K. Srai, A.T. McKie, P.A. Sharp, Hypoxia inhibits hepcidin expression in HuH7 hepatoma cells via decreased SMAD4 signaling, Am. J. Physiol. Cell Physiol. 300 (4) (2011) C888–C895.
[26] R. Nakatsuka, M. Taniguchi, M. Hirata, G. Shiota, K. Sato, Transient expression of bone morphogenic protein-2 in acute liver injury by carbon tetrachloride, J. Biochem. 141 (1) (2007) 113–119.
[27] N. Oumi, K.A. Taniguchi, A.M. Kanai, M. Yasunaga, T. Nakanishi, K. Sato, A crucial role of bone morphogenetic protein signaling in the wound healing response in acute liver injury induced by carbon tetrachloride, Int J Hepatol 2012 (2012) 476820.
[28] A. Stavropoulos, G. Divolis, M. Manioudaki, A. Gavriil, I. Kloukina, D.N. Perrea, et al., Coordinated activation of TGF-β and BMP pathways promotes autophagy and limits liver injury after acetaminophen intoxication, Sci. Signal. 15 (740) (2022) eabn4395.
[29] A. González-Rodríguez, J.A. Mas Gutierrez, S. Sanz-González, M. Ros, D.J. Burks, A.M. Valverde, Inhibition of PTP1B restores IRS1-mediated hepatic insulin signaling in IRS2-deficient mice, Diabetes 59 (3) (2010) 588–599.
[30] M.A. Mobasher, A. González-Rodriguez, B. Santamaría, S. Ramos, M. Martín, L. Goya, et al., Protein tyrosine phosphatase 1B modulates GSK3β/Nrf 2 and IGFIR signaling pathways in acetaminophen-induced hepatotoxicity, Cell Death Dis. 4 (5) (2013) e626.
[31] M.A. Mobasher, J. de Toro-Martín, Á. González-Rodríguez, S. Ramos, L.G. Letzig, L. P. James, et al., Essential role of protein-tyrosine phosphatase 1B in the modulation of insulin signaling by acetaminophen in hepatocytes, J. Biol. Chem. 289 (42) (2014) 29406–29419.
[32] H. Ye, C. Chen, H. Wu, K. Zheng, B. Martín-Adrados, E. Caparros, et al., Genetic and pharmacological inhibition of XBP1 protects against APAP hepatotoxicity through the activation of autophagy, Cell Death Dis. 13 (2) (2022) 143.
[33] D.J. Augeri, E. Langenfeld, M. Castle, J.A. Gilleran, J. Langenfeld, Inhibition of BMP and of TGFβ receptors downregulates expression of XIAP and TAK1 leading to lung cancer cell death, Mol. Cancer 15 (2016) 27.
[34] D. Tsugawa, Y. Oya, R. Masuzaki, K. Ray, D.W. Engers, M. Dib, et al., Specific activin receptor-like kinase 3 inhibitors enhance liver regeneration, J. Pharmacol. Exp. Therapeut. 351 (3) (2014) 549–558.
[35] E.G. Worthley, C.D. Schott, The toxicity of four concentrations of DMSO, Toxicol. Appl. Pharmacol. 15 (2) (1969) 275–281.
[36] I. Cordero-Herrera, M.A. Martín, L. Goya, S. Ramos, Cocoa flavonoids protect hepatic cells against high-glucose-induced oxidative stress: relevance of MAPKs, Mol. Nutr. Food Res. 59 (4) (2015) 597–609.
[37] A.B. Reid, R.C. Kurten, S.S. McCullough, R.W. Brock, J.A. Hinson, Mechanisms of acetaminophen-induced hepatotoxicity: role of oxidative stress and mitochondrial permeability transition in freshly isolated mouse hepatocytes, J. Pharmacol. Exp. Therapeut. 312 (2) (2005) 509–516.

[38] Y.T. Xiao, L.X. Xiang, J.Z. Shao, Bone morphogenetic protein, Biochem. Biophys. Res. Commun. 362 (3) (2007) 550–553.
[39] M.L. Zou, Z.H. Chen, Y.Y. Teng, S.Y. Liu, Y. Jia, K.W. Zhang, et al., The Smad dependent TGF-β and BMP signaling pathway in bone remodeling and therapies, Front. Mol. Biosci. 8 (2021) 593310.
[40] K. Yamaguchi, S. Nagai, J. Ninomiya-Tsuji, M. Nishita, K. Tamai, K. Irie, et al., XIAP, a cellular member of the inhibitor of apoptosis protein family, links the receptors to TAB1-TAK1 in the BMP signaling pathway, EMBO J. 18 (1) (1999) 179–187.
[41] Z. Liang, B. Wu, Z. Ji, W. Liu, D. Shi, X. Chen, et al., The binding of LDN193189 to CD133 C-terminus suppresses the tumorigenesis and immune escape of liver tumor-initiating cells, Cancer Lett. 513 (2021) 90–100.
[42] T.E. Thayer, C.L. Lino Cardenas, T. Martyn, C.J. Nicholson, L. Traeger, F. Wunderer, et al., The role of bone morphogenetic protein signaling in non-alcoholic fatty liver disease, Sci. Rep. 10 (1) (2020) 9831.